# SUPPORTING INFORMATION

# Dynamics of the Excited State of $[Ir(ppy)_2bpy]^+$ with triple Phosphorescence

*Shih-Hsiang Wu, Jung-Wei Ling, Szu-Hsueh Lai, Min-Jie Huang, Chien Hong Cheng, and I-Chia Chen**

*Department of Chemistry, National Tsing Hua University, Hsinchu, Taiwan 30013,*

*Republic of China*

**SUPPORTING INFORMATION:** the optimized geometry of $[Ir(ppy)_2bpy]^+$, emission curves of $[Ir(ppy)_2bpy]^+$ at excitation wavelength 355 nm in various solvents and the best-fitted exponential curves and picosecond measurements on decay curves of $[Ir(ppy)_2bpy]^+$ in toluene/$CHCl_3$ volume ratio 1:1 and $CHCl_3$.

**Captions of figures**

**Figure S1.** Optimized geometry of $[Ir(ppy)_2bpy]^+$ calculated at level B3LYP/6-31G* restricted to symmetry $C_2$. The bond distance of Ir-C and Ir-N is 2.028 Å and 2.085 Å, respectively to ppy. The bond distances of C-C in ppy are ~1.460Å and the dihedral angle C-C-C-N is 1.3°. The bond distance of Ir-N is 2.211 Å to bpy. The bond distances of C-C in bpy are ~1.483Å and the dihedral angle N-C-C-N is 4°.

**Figure S2.** Emission curves of $[Ir(ppy)_2bpy]^+$ at excitation wavelength 355 nm and detected at wavelength 500 and 580 nm in toluene and the best-fitted exponential curves.

**Figure S3.** Emission curves of $[Ir(ppy)_2bpy]^+$ at excitation wavelength 355 nm and detected at wavelength 500 and 580 nm in toluene/$CHCl_3$ at volume ratio 1:1 and the best-fitted exponential curves.

**Figure S4.** Emission curves of $[Ir(ppy)_2bpy]^+$ at excitation wavelength 355 nm and detected at wavelength 500 and 580 nm in $CHCl_3$ and the best-fitted exponential curves.

**Figure S5.** Emission curves of $[Ir(ppy)_2bpy]^+$ at excitation wavelength 355 nm and detected at wavelength 500 and 580 nm in THF and the best-fitted exponential curves.

**Figure S6.** Emission curves of $[Ir(ppy)_2bpy]^+$ at excitation wavelength 355 nm and detected at wavelength 500 and 580 nm in $CH_2Cl_2$ and the best-fitted exponential curves.

**Figure S7.** Emission curves of $[Ir(ppy)_2bpy]^+$ at excitation wavelength 355 nm and detected at wavelength 500 and 580 nm in acetone and the best-fitted exponential curves.

**Figure S8.** Emission curves of $[Ir(ppy)_2bpy]^+$ at excitation wavelength 355 nm and detected at wavelength 500 and 580 nm in acetonitrile and the best-fitted exponential curves.

**Figure S9.** Emission curves of $[Ir(ppy)_2bpy]^+$ at excitation wavelength 355 nm and detected at wavelength 500 and 580 nm in DMF and the best-fitted exponential curves.

**Figure S10.** Emission curves of $[Ir(ppy)_2bpy]^+$ at excitation wavelength 355 nm and detected at wavelength 500 and 580 nm in DMSO and the best-fitted exponential curves.

**Figure S11.** Emission decay curves of $[Ir(ppy)_2bpy]^+$ in toluene/$CHCl_3$ volume ratio 1:1 excited at wavelength 355 nm.

**Figure S12.** Emission decay curves of $[Ir(ppy)_2bpy]^+$ in $CHCl_3$ excited at wavelength 355 nm.

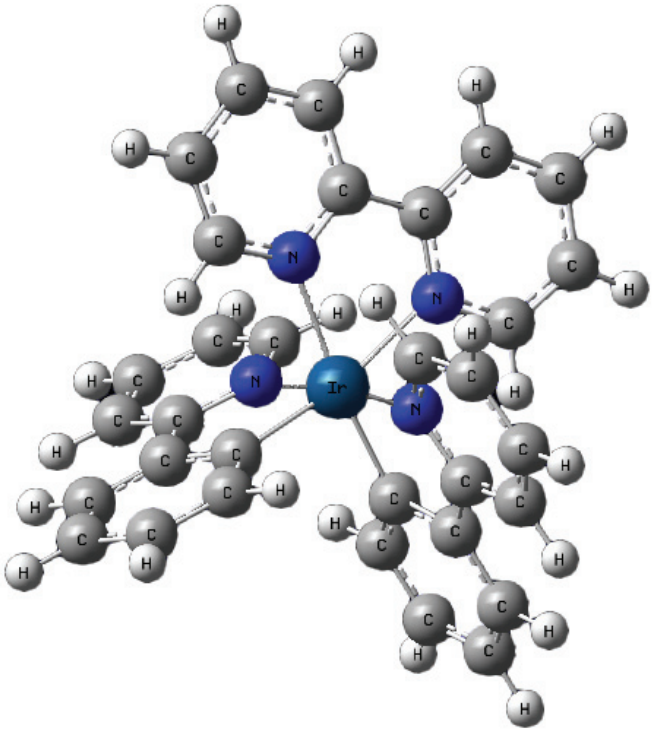

**Figure S1.** Optimized geometry of $[Ir(ppy)_2bpy]^+$ calculated at level B3LYP/6-31G* restricted to symmetry $C_2$. The bond distance of Ir-C and Ir-N is 2.028 Å and 2.085 Å, respectively to ppy. The bond distances of C-C in ppy are ~1.460Å and the dihedral angle C-C-C-N is 1.3°. The bond distance of Ir-N is 2.211 Å to bpy. The bond distances of C-C in bpy are ~1.483Å and the dihedral angle N-C-C-N is 4°.

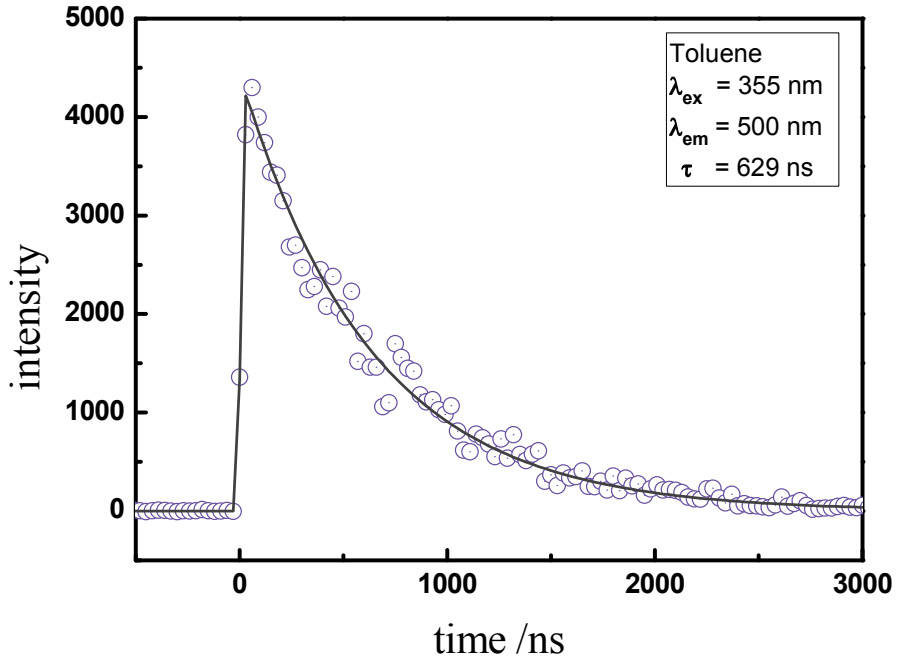


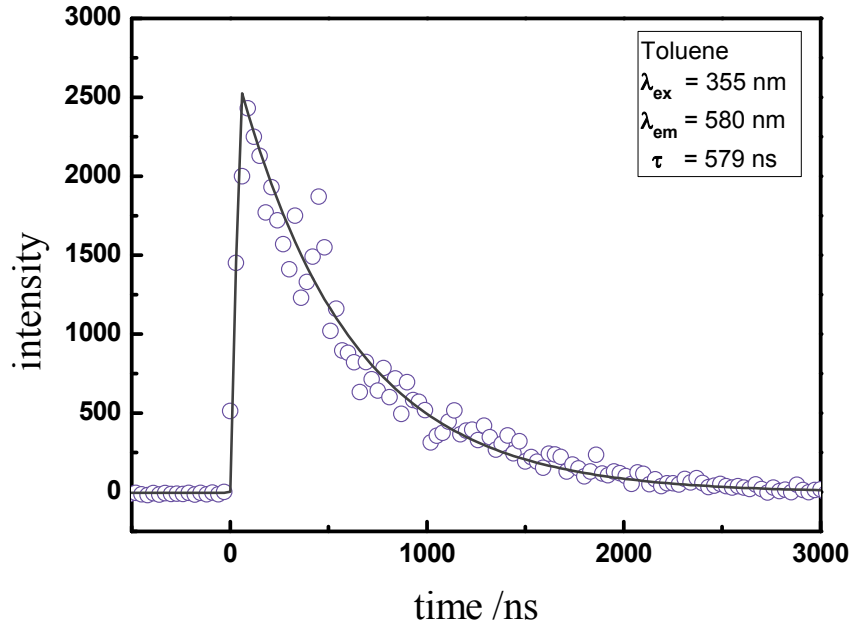


Figure S2. Emission curves of $[Ir(ppy)_2bpy]^+$ at excitation wavelength 355 nm and detected at wavelength 500 and 580 nm in toluene and the best-fitted exponential decay curves.

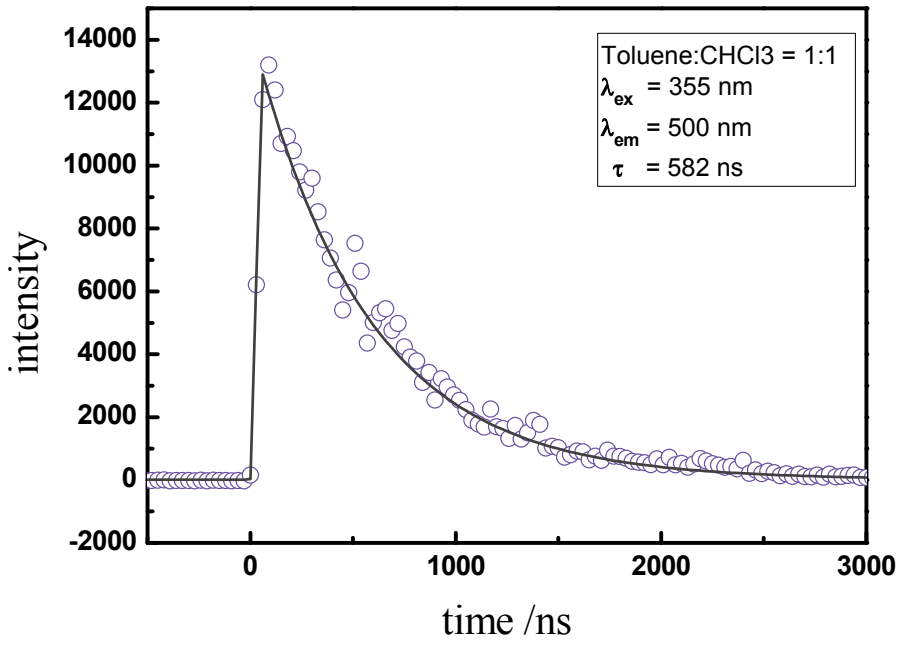


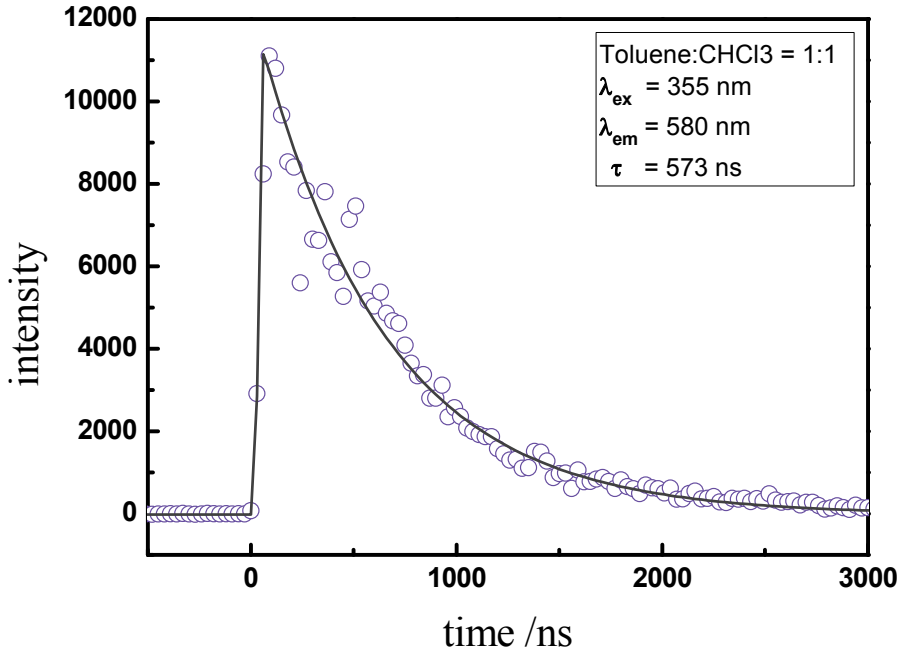


Figure S3. Emission curves of $[Ir(ppy)_2bpy]^+$ at excitation wavelength 355 nm and detected at wavelength 500 and 580 nm in toluene/$CHCl_3$ at volume ratio 1:1 and the best-fitted exponential curves.

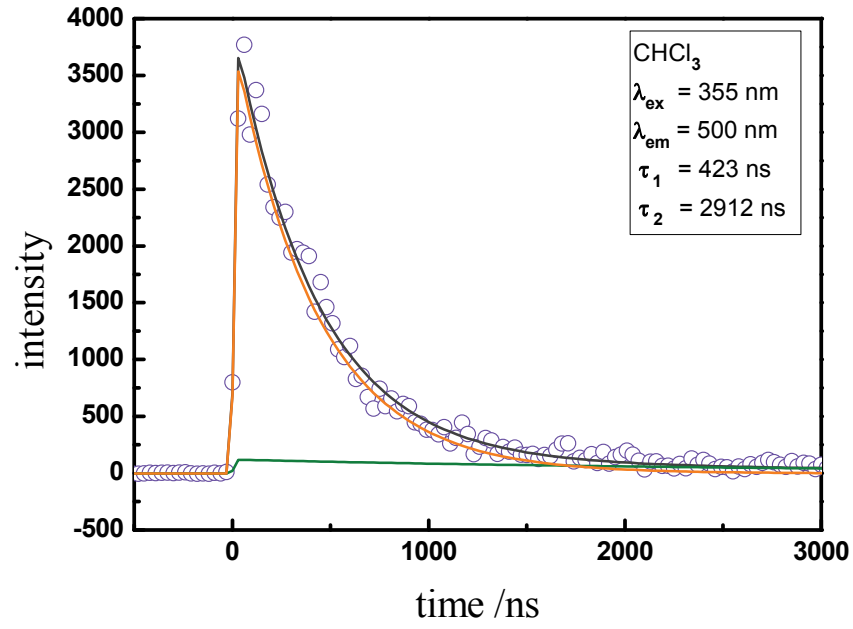


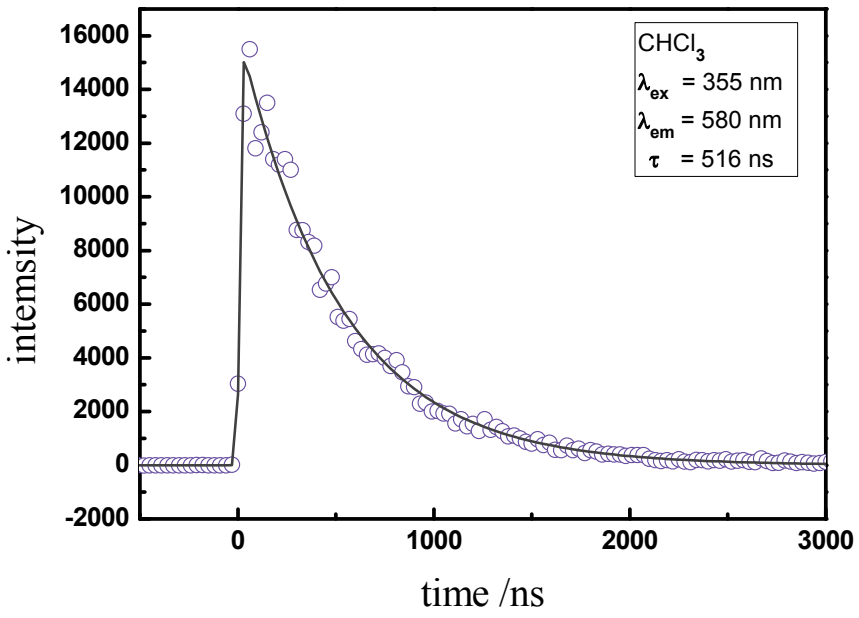


Figure S4. Emission curves of $[Ir(ppy)_2bpy]^+$ at excitation wavelength 355 nm and detected at wavelength 500 and 580 nm in $CHCl_3$ and the best-fitted exponential curves.

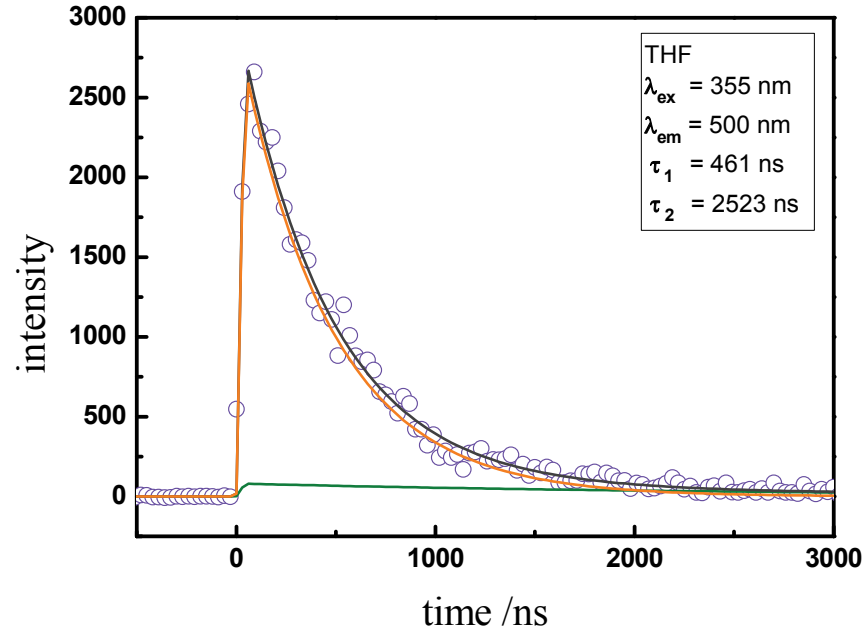


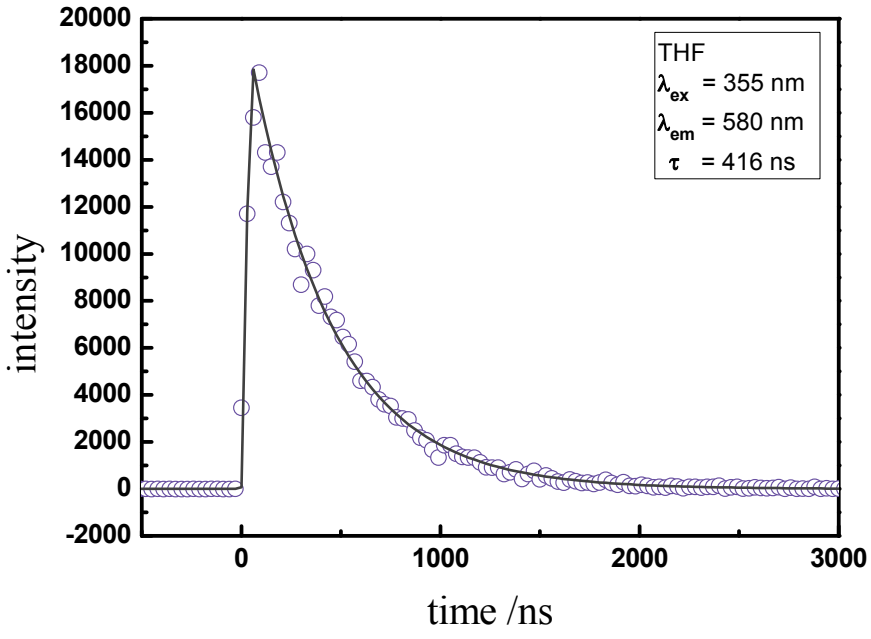


Figure S5. Emission curves of $[Ir(ppy)_2bpy]^+$ at excitation wavelength 355 nm and detected at wavelength 500 and 580 nm in THF and the best-fitted exponential curves.

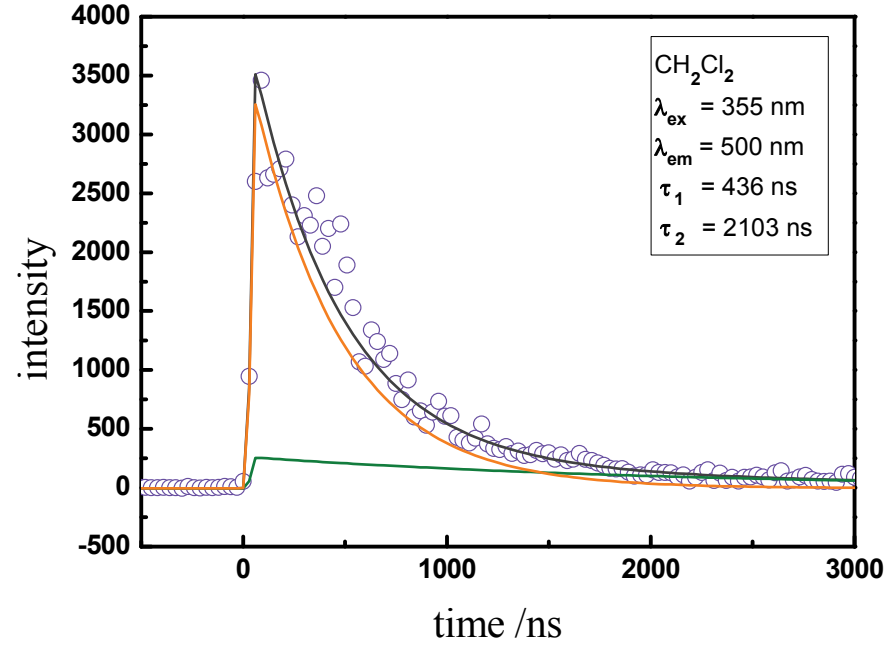


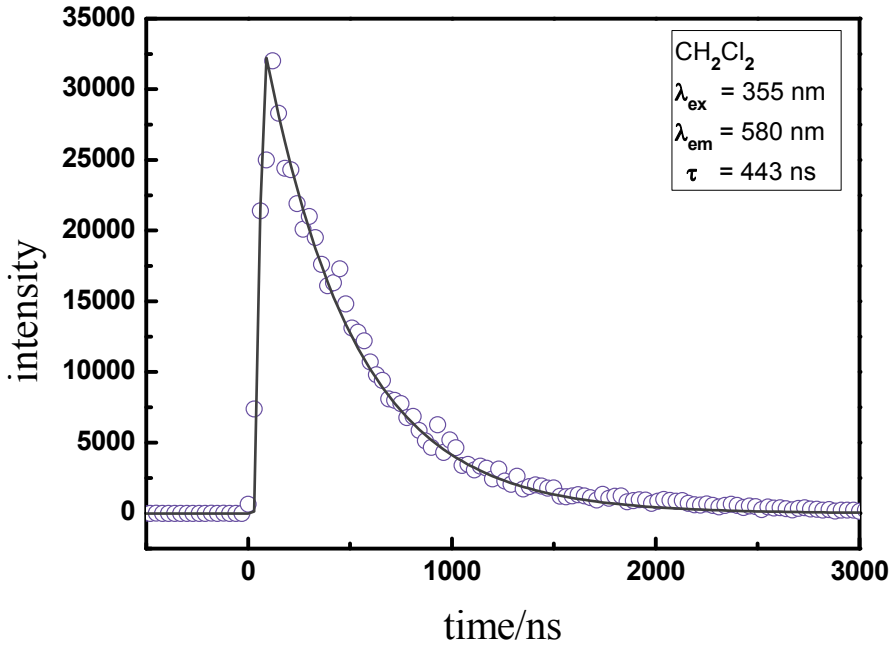


Figure S6. Emission curves of $[Ir(ppy)_2bpy]^+$ at excitation wavelength 355 nm and detected at wavelength 500 and 580 nm in $CH_2Cl_2$ and the best-fitted exponential curves.

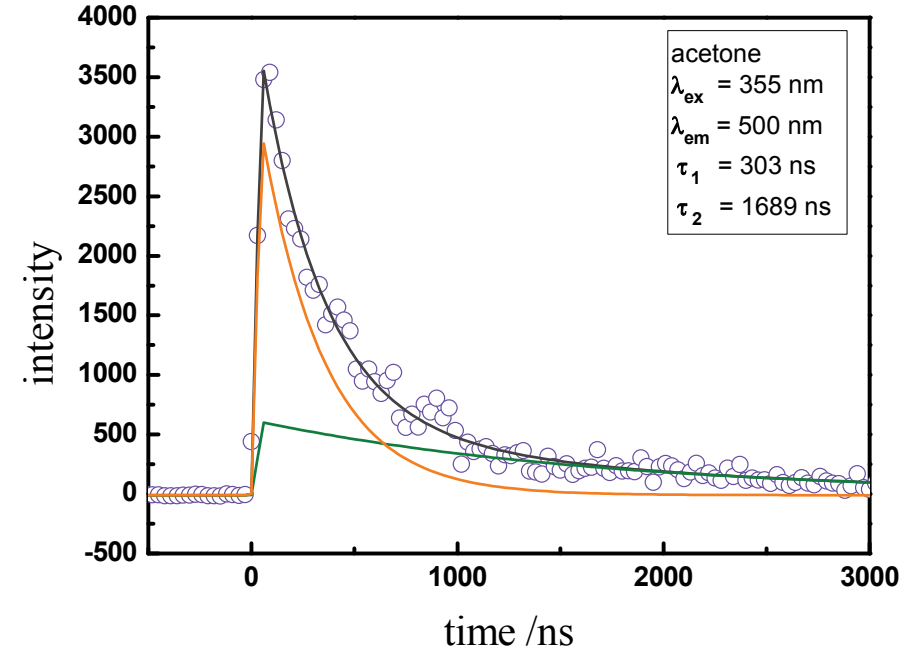


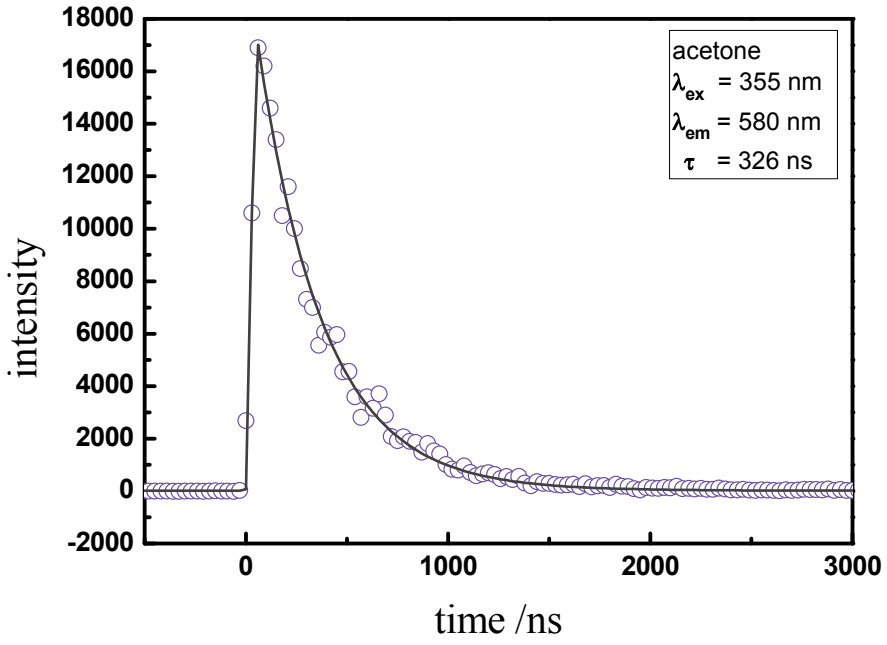


Figure S7. Emission curves of $[Ir(ppy)_2bpy]^+$ at excitation wavelength 355 nm and detected at wavelength 500 and 580 nm in acetone and the best-fitted exponential curves.

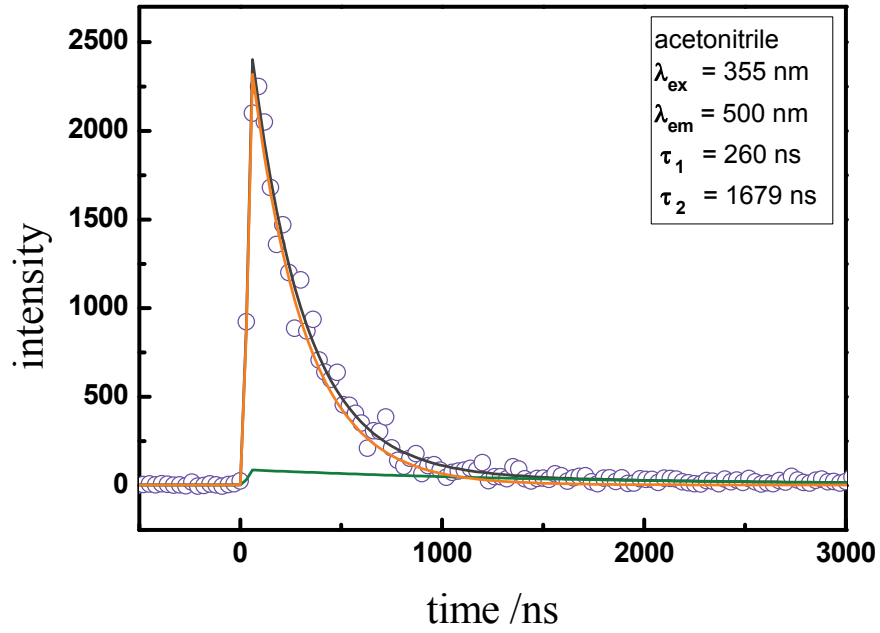


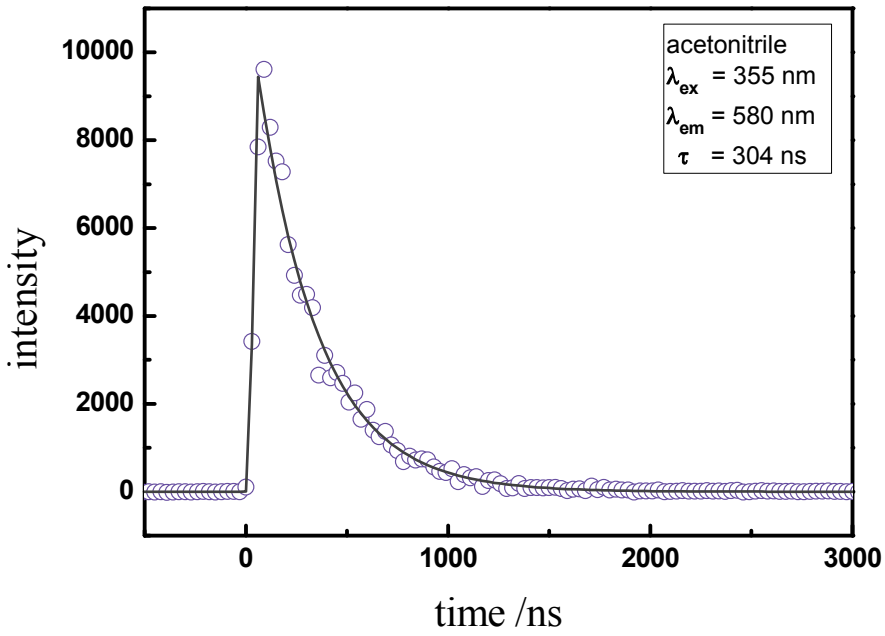


Figure S8. Emission curves of $[Ir(ppy)_2bpy]^+$ at excitation wavelength 355 nm and detected at wavelength 500 and 580 nm in acetonitrile and the best-fitted exponential curves.

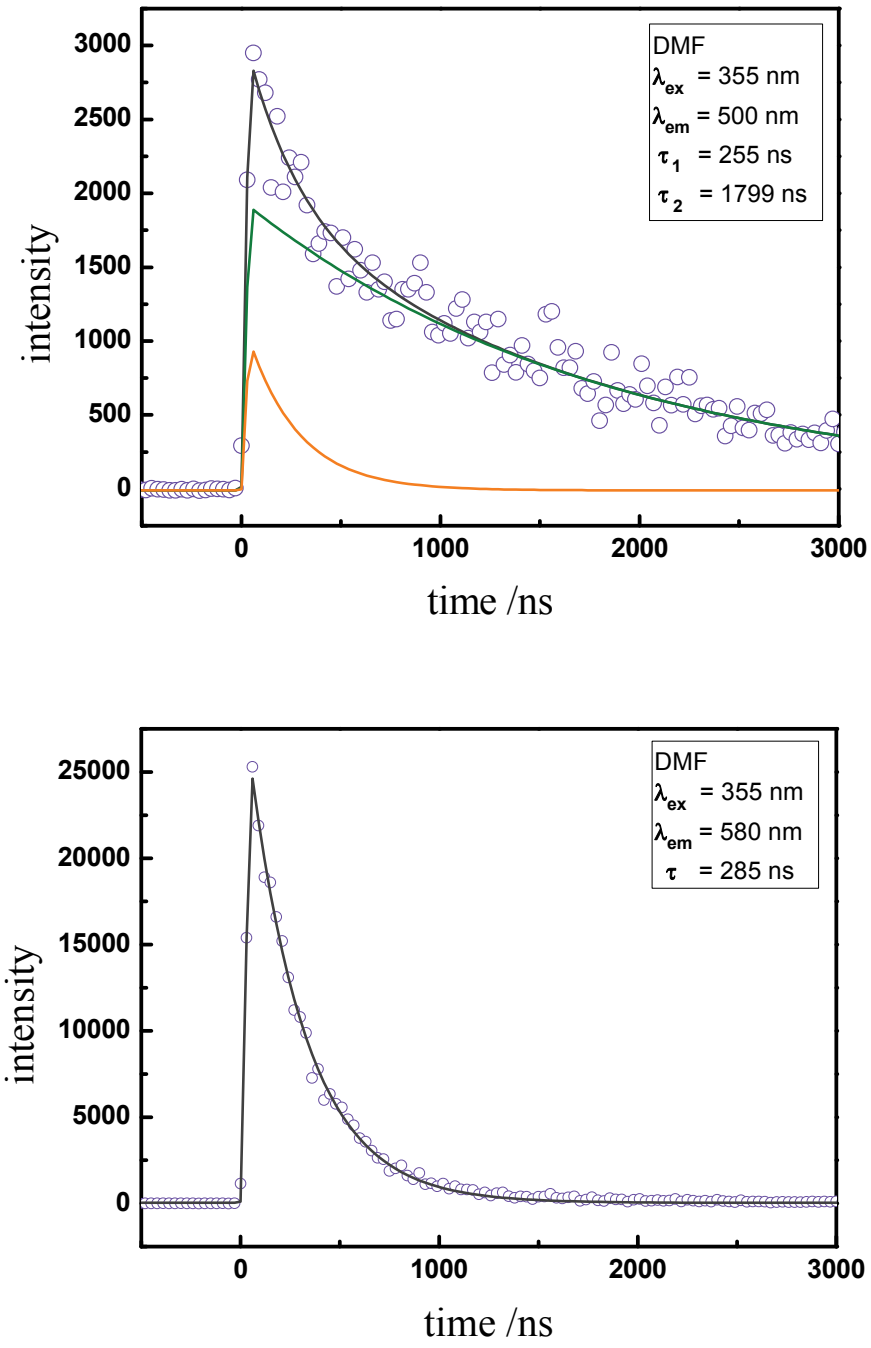


Figure S9. Emission curves of $[Ir(ppy)_2bpy]^+$ at excitation wavelength 355 nm and detected at wavelength 500 and 580 nm in DMF and the best-fitted exponential curves.

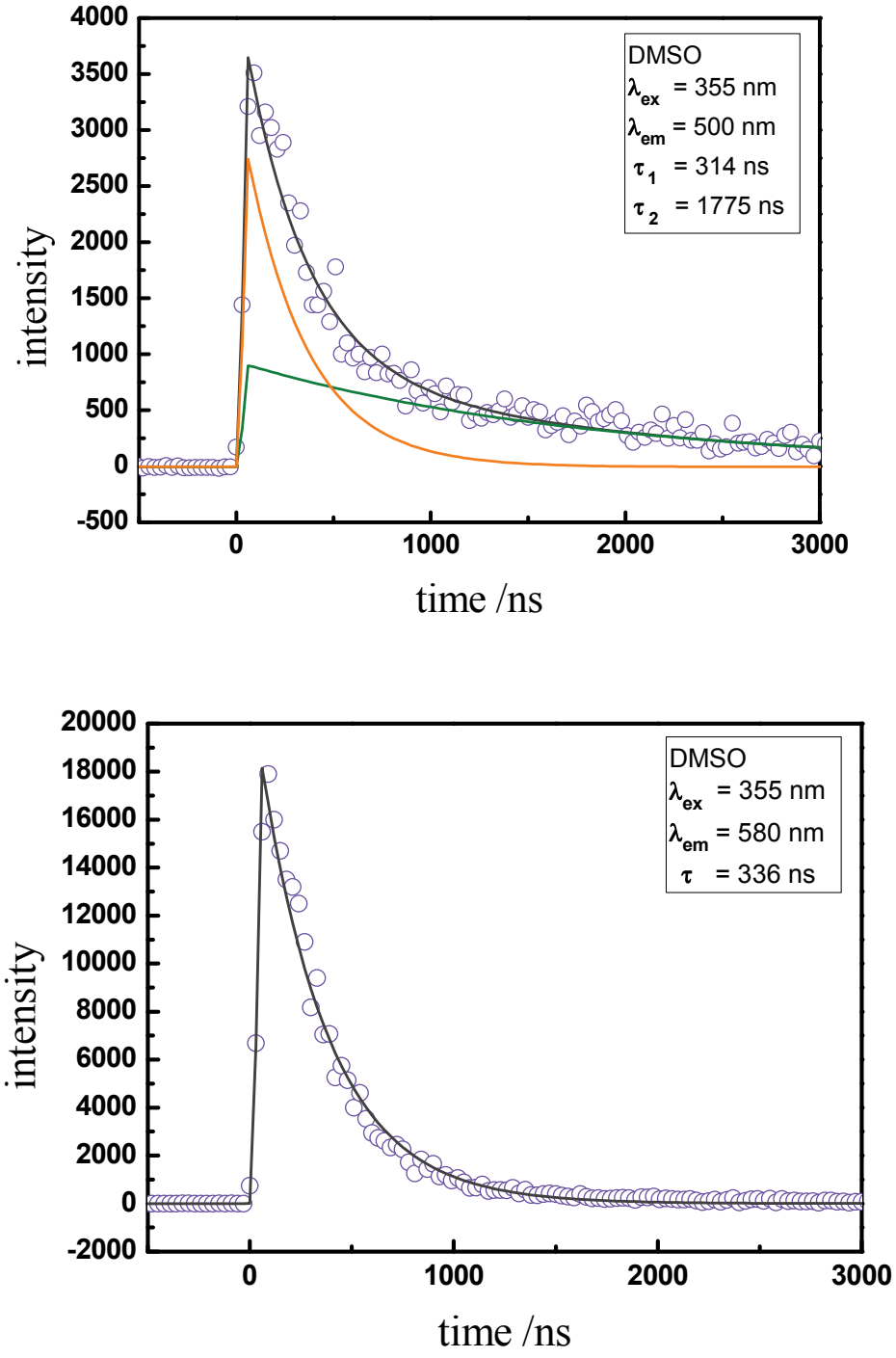


Figure S10. Emission curves of $[Ir(ppy)_2bpy]^+$ at excitation wavelength 355 nm and detected at wavelength 500 and 580 nm in DMSO and the best-fitted exponential curves.

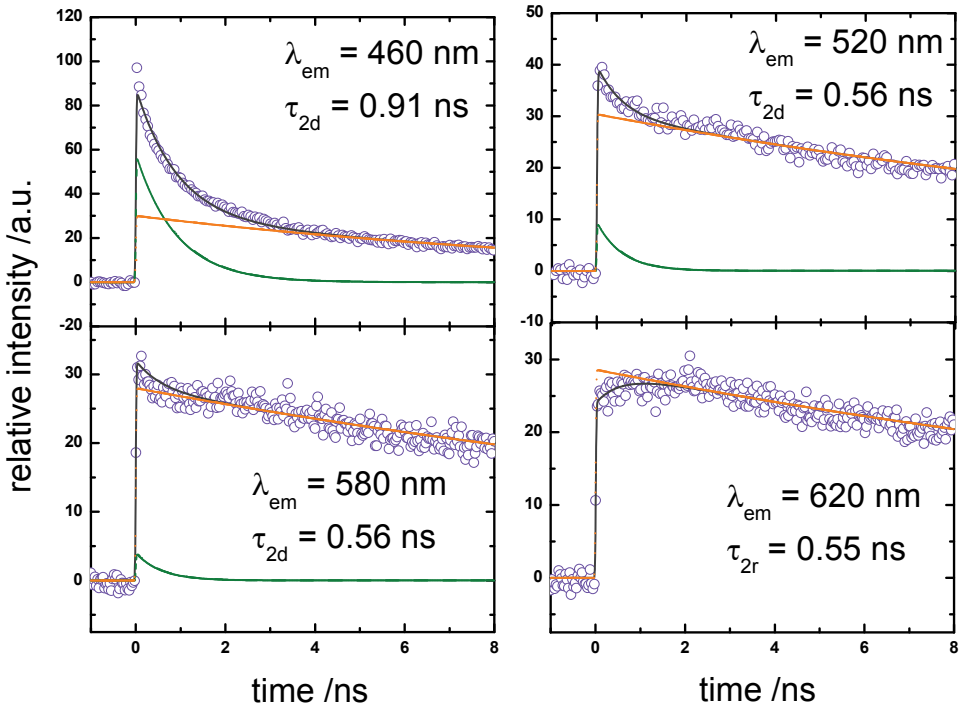


Figure S11. Emission decay curves of $[Ir(ppy)_2bpy]^+$ in toluene/$CHCl_3$ volume ratio 1:1 excited at wavelength 355 nm.

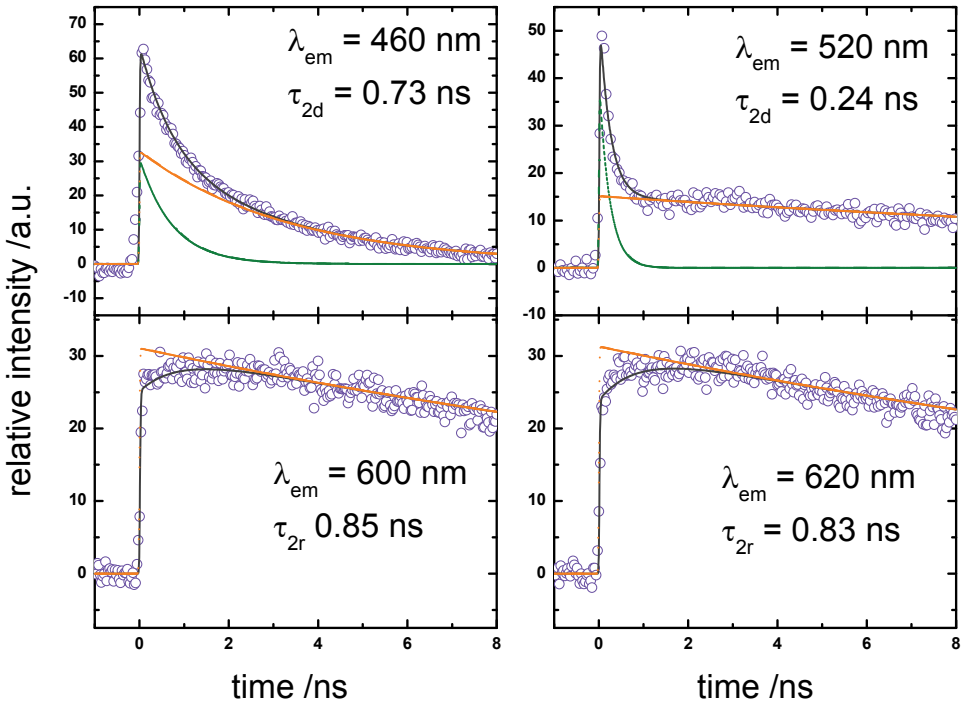


Figure S12. Emission decay curves of $[Ir(ppy)_2bpy]^+$ in $CHCl_3$ excited at wavelength 355 nm.